UNIVERSITÀ POLITECNICA DELLE MARCHE
Repository ISTITUZIONALE

Reverberation chambers for testing wireless devices and systems

This is the peer reviewd version of the followng article:

Original
Reverberation chambers for testing wireless devices and systems / Mariani Primiani, V.; Barazzetta, M.; Bastianelli, L.; Micheli, D.; Moglie, F.; Diamanti, R.; Gradoni, G.. - In: IEEE ELECTROMAGNETIC COMPATIBILITY MAGAZINE. - ISSN 2162-2264. - ELETTRONICO. - 9:2(2020), pp. 45-55. [10.1109/MEMC.2020.9133241]

Availability:
This version is available at: 11566/307343 since: 2024-04-24T11:29:59Z

Publisher:

Published
DOI:10.1109/MEMC.2020.9133241

Terms of use:

The terms and conditions for the reuse of this version of the manuscript are specified in the publishing policy. The use of copyrighted works requires the consent of the rights' holder (author or publisher). Works made available under a Creative Commons license or a Publisher's custom-made license can be used according to the terms and conditions contained therein. See editor's website for further information and terms and conditions.
This item was downloaded from IRIS Università Politecnica delle Marche (https://iris.univpm.it). When citing, please refer to the published version.

note finali coverpage

(Article begins on next page)

25 August 2024

POST PRINT VERSION

DOI: 10.1109/MEMC.2020.9133241

Editor Website: https://ieeexplore.ieee.org/abstract/document/9133241

Title: Reverberation chambers for testing wireless devices and systems

Publication: IEEE Electromagnetic Compatibility Magazine

Publisher: IEEE

Date: 2nd Quarter 2020

© 2020 IEEE. Personal use of this material is permitted. Permission from IEEE must be obtained for all other uses, in any current or future media, including reprinting/republishing this material for advertising or promotional purposes, creating new collective works, for resale or redistribution to servers or lists, or reuse of any copyrighted component of this work in other works.

Reverberation chambers for testing wireless devices and systems

V. Mariani Primiani[(1)], M. Barazzetta[(2)], L. Bastianelli[(1)], D. Micheli[(3)], F. Moglie[(1)], R. Diamanti[(3)], G. Gradoni[(4)]

[(1)]Università Politecnica delle Marche – DII- Ancona – Italy

valter.mariani@univpm.it

(2) Nokia Networks – Vimercate -Italy

[(3)]TIM S.p.A.- Roma- Italy

[(4)]University of Nottingham – United Kingdom

Abstract Testing of wireless devices and systems is becoming increasingly important in the technological development of Long Term Evolution (LTE) and 5G mobile networks. Both mobile and base station manufacturers are interested in assessing system performance and user perceived quality in realistic propagation environments, including indoor and outdoor conditions. Real-life electromagnetic environments exhibit rich multipath propagation and a strong attenuation of the wireless signal over the propagation channel. Emulating those conditions in anechoic chambers requires the careful arrangement of many interference sources in multiple configurations, which leads to complex and time-consuming measurements. The reverberation chamber (RC) is a metallic cavity where the signal created by a single source is reflected and diffused to create multipath fading. This paper gives an overview of how an RC can be tuned to emulate channel parameters, e.g., power delay profile, time delay spread, coherence bandwidth and Rician K-factor, of real-life environments The addition of absorbing material inside the RC allows for varying those parameters, thus recreating line of sight and imperfect propagation conditions experienced by the user equipment (UE). Compliant electromagnetic compatibility downlink and uplink tests are shown for selected MIMO configurations as well as for Internet of Things devices. The tests are carried out using a commercial base station connected to the live national mobile network of a mobile operator. Evaluated network parameters are throughput, signal to noise ratio, modulation schemes and other settings of both the base station and of the UE to assess the quality of the digital communication.

1 INTRODUCTION

Reverberation chambers (RCs) are resonant enclosures that operate at a frequency where a large amount of modes are excited at the same time. This overmoded condition contributes to the establishment of a field inside the chamber that is statistically uniform, isotropic and without a preferable polarization [1]. The stochastic nature of the RC's electromagnetic field [2] is useful in electromagnetic compatibility (EMC) testing [3], material characterization [4] also including shielding effectiveness [5] antenna characterization [6]-[7], and for the assessment of human exposure to electromagnetic fields [8]. Assuming wireless communication systems operating into a real environment, they face very complex propagation conditions, made of many reflections that can become strongly uncorrelated in urban and indoor environment, due to the presence of moving scattering objects and people. These real propagation conditions are more similar to what happens inside an RC w.r.t. an anechoic chamber adopted in classical tests. RC is used to reproduce different propagation environments by controlling the multipath amount [9], [10] and radio with no unwanted effects of external interfering signals. The emulation of a Rician environment can be done by a single [11] or coupled RCs [12]-[13], also accounting for the antenna behavior in this kind of propagation [14]. The multipath degree of the RC is varied by inserting absorbing materials, so tuning it from a typical indoor environment up to an extreme reflecting place [15]–[16]. Beside the classical characterization of the RC statistical properties [17]–[18], in order to correctly perform wireless tests, e.g. about devices or propagation condition and so on, it is required a different assessment for the uncertainty components [19]–[20]. Moreover, the adopted stirring method [21] influence the uncertainty, so suggesting the development of new stirring techniques [22].
Complete over-the-air (OTA) tests are carried out [23]-[24] on wireless local area network [25], for OTA testing on long term evolution (LTE) terminals [26]-[28] and real base station (BS) to check terms of throughput (TP)

,

under hostile conditions in both downlink [27] and uplink [29] directions. The RC can also be successfully used to replicate user quality perception on board of high speed train [30]. In fact, inside high speed train coaches, each of them similar to a metallic enclosure, there are a large number of terminals that operate simultaneously. They share the connection to the BS with a relatively very high velocity that introduces a Doppler shift effect too.

2. REAL LIFE PROPAGATION CHANNELS

A real life wireless communication scenario is made by many reflections. Those reflections create very complex propagation conditions. Reflections are generated by different sources, e.g. buildings, cars, walls, etc, and by different phenomenon, see respectively Fig .1.

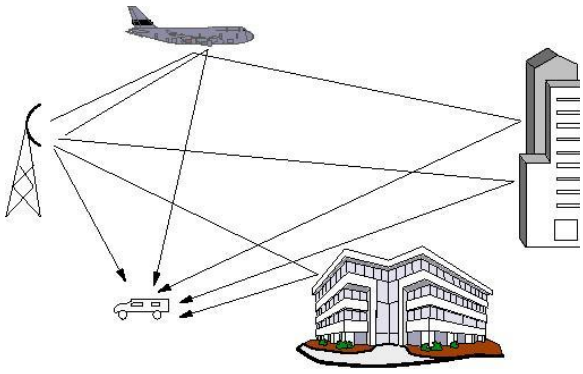

Figure 1. Real life multipath propagation channel.

From an electromagnetic point of view, this complex scenario gives rise to a multiple excitation of the user equipment (UE) due to a summation of signal delayed in time and having a different shape according to what they encounter during the flight between the BS and the reception point.
In the frequency domain, this means that the signal received at any point in the environment might be thought as the summation of a direct link between the BS and the UE plus the presence of many other contribution due to the reflection, diffraction and scattering determined by objects having different conductivity and shape.
The combination of a direct signal between the transmitting antenna, line-of-sight (LOS), and a scattered component, non-line-of-sight (NLOS), determines a particular characteristic of the received signal. It is characterized by strong time and space fluctuations with respect to a mean value [32].
In a rural environment, the BS is usually in LOS, therefore the direct component is stronger than the diffused one and deep minimum are less likable. On the contrary, in an urban situation the probability to have a visibility on the BS is lower, and the field is largely given diffused component due to buildings, buses, cars and so on. In that situation, the multipath components may combine in phase and out of phase so giving deep signal minima. Moreover, in an urban environment the UE faces a dynamic condition due to moving reflecting objects, as well as when the UE is on board of cars or trains. The balancing between the LOS and the NLOS component is defined by the so called Rician K-factor [33].

$$K = \frac{directcomponent}{scatteredcomponent} \qquad (1)$$

In this conditions, the probability distribution function of the collected received signal samples yields a Rician distribution [11]

$$f(|E_x|) = \frac{|E_x|}{\sigma^2} e^{\frac{-(|E_x|^2+|E_{xd}|^2)}{2\sigma^2}} I_0\left(\frac{|E_x||E_{xd}|}{\sigma^2}\right) \qquad (2)$$

,

where $E_x = E_{xs} + E_{xd}$ is a Cartesian field component made of a scattered contribution E_{xs} plus a direct one E_{xd}, and the scattered contribution is made by a real and an imaginary part both normally distributed with equal variance σ^2 and uncorrelated to each other, $E_{xs} = E_{xsr} + jE_{xsi}$.
$I_0$is the modified Bessel function of zero order.

It is characterized by two parameters which reflect the definition of the K factor

$$K = \frac{|E_{xd}|^2}{2\sigma^2}. \tag{3}$$

Given these propagation characteristics, testing wireless devices in a reflecting environment becomes of practical importance [34].
Emulating those conditions in anechoic chambers requires the careful arrangement of many interference sources in multiple configurations, which leads to complex and time-consuming measurements. In fact, an approximation of the real life situation is achieved by adopting a limited number of delayed taps, as suggested by Standards [35, table B2-1-1-1], whereas the RC provides infinite taps with whatever amplitude and delay at a lower cost.

3 REVERBERATION CHAMBER

The multipath propagation characteristic of a real environment is intrinsically available inside an RC. It is an electrically large cavity, whose highly reflecting walls generate a rich multipath propagation for a launched signal, Fig. 2.

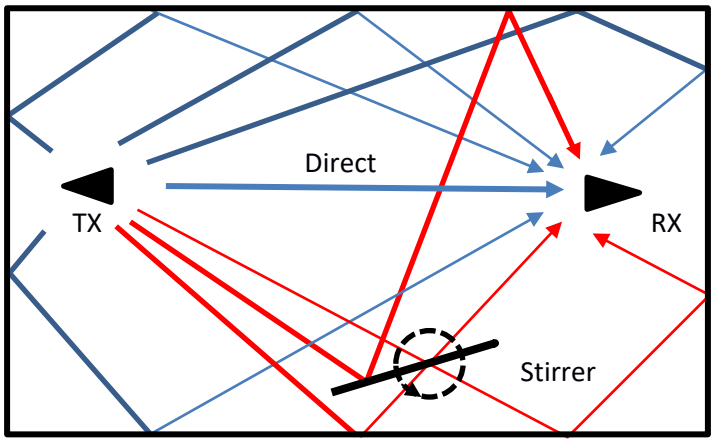

Figure 2: Multipath propagation in an RC. The rotating stirrer acts on the amount of the scattered component.

Due to the large amount of excited modes, the receiving antenna can be exposed to different field levels according to its position inside the chamber, as happens for a UE in a real environment, Fig. 3 [37]. The figure also shows in the inset the electric field amplitude pattern computed at 1 GHz: the chaotic nature of the field spatial variation is evident through the colored map.

,

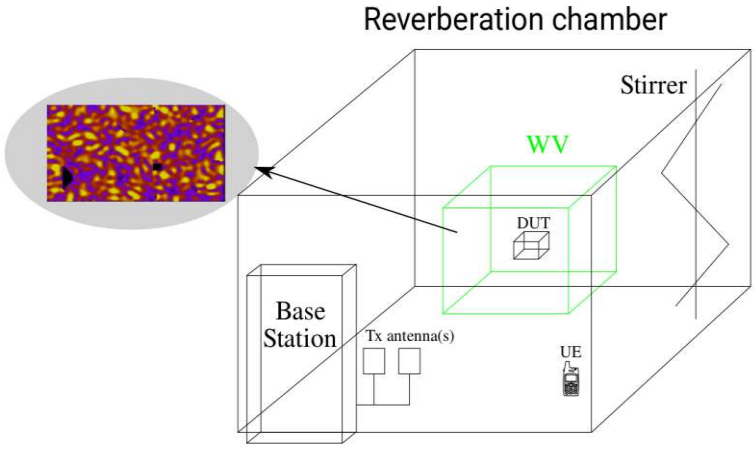

Figure 3: A 6 x 4 x 2.5 m^3reverberation chamber equipped by a LTE base station, MIMO transmitting antennas, and equipment under tests. The inset shows the field chaoticity within the RC [36].

An example of the capability of the RC to replicate real conditions can be found in [30 (Fig. 5)], where the signal fluctuations measured on board a high speed train were compared to those obtained inside an RC for a chosen stirrer rotating speed, Fig. 4. Fluctuations exhibit a similar excursion and a similar random behavior.

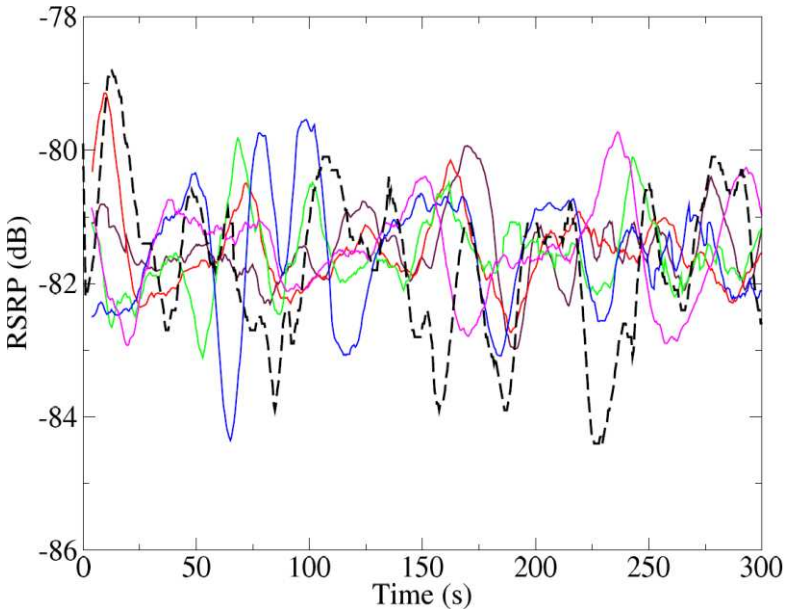

Fig. 4. UE received signal fluctuations inside a high speed train coach for different positions (colored lines) compared to that reproduced inside an RC by a proper stirrer rotating speed (dashed black line). Curtesy from [30]

,

RC is widely used for EMC tests. The RC provides a statistically uniform, isotropic and depolarized field within a defined region, called working volume [1]. These properties are achieved after a proper stirring process able to change the field characteristics in each chamber location according to a prefixed distribution function. In that way, the device under test can be kept at a fixed position and exposed to variable field levels.
The stirring action can be accomplished by mechanical methods or/and electronic methods. Mechanical stirring is obtained by rotating metallic paddles or by moving or vibrating the chamber walls. Electronic stirring can be done by varying the frequency and or the amplitude of the injected signal or by changing the position of the transmitting antennas. A comprehensive description of main stirring methods can be found in [38].
The goodness of a RC for EMC tests is checked by computing some performance indicators capable to quantify the amount of uniformity and randomness of the field under the adopted stirring action. A list of typical performance indicators and their typical values can be found in [39].
Each Cartesian component of the field inside a well operating RC has a real and an imaginary part normally-distributed with zero mean value, equal variances and uncorrelated with each other. As a consequence, the amplitude of each Cartesian component, for example E_x, has a Rayleigh distribution when field samples are collected over a complete cycle of the stirring process (mechanical or electronic) [2], [7], [11]

$$f(|E_x|) = \frac{|E_x|}{\sigma^2} e^{\frac{-|E_x|^2}{2\sigma^2}} \qquad (4)$$

For EMC testing, this can be accomplished by reducing as much as possible the direct path visible in Figure 2, by a proper positioning of the TX antenna and of the stirrer. On the contrary, for wireless device testing the direct path is restored. This is a key aspect, because the RC is intrinsically characterized by a rich multipath, but the probability distribution function of each propagating environment differs from each other. Therefore, in order to use an RC for testing wireless system it is necessary to degrade its performance passing from an ideally operating chamber to a non-ideal one described by a Rician distribution [32].
The Rician K-factor inside an RC can be tuned from very low levels (order of 10^{-2} for a good RC) to higher values similar to what encountered in realistic propagation environment. This is done by varying the ratio between the direct component and the scattered one. To do that, different actions can be taken according to the following simple relationship [33], [40]

$$K = \frac{3}{2}\frac{V}{\lambda Q}\frac{D}{r^2} \qquad (5)$$

where V is the chamber volume, Q is the chamber quality factor, D is the antenna directivity, r is the distance between the transmitting and receiving antennas, and λ is the wavelength at the operating frequency.
An example of RC set up where the K factor is tuned to a wanted value is shown in Fig. 5.

Figure 5: A typical outdoor antenna element for the 800 MHz and 1800 MHz LTE band brings a base station signal inside the RC. It is located a distance r from the UE (a dongle connected to a notebook), and some absorbing pyramidal and planar absorbers are put inside the RC.

,

The antenna orientation can be changed to vary the directivity toward the UE, to vary the amplitude of the direct illumination. The distance between the antenna and the UE can be varied to reduce or to increase the direct component. Finally, the addition of absorbing materials reduces the chamber quality factor.
As an example, Fig. 6 reports the quality factor computed for an RC having dimensions 6x4x2.5 m^3 equipped by a vertical z-folded stirrer, as function of the number of inserted absorbers and according to [37], [41], see Table I:

$$Q = \frac{16\pi^2 V}{\eta_{Tx}\eta_{Rx}\lambda^3}\left\langle \frac{P_{ave,rec}}{P_{input}} \right\rangle_N \tag{6}$$

where P_{input} is the net power delivered to the RC, P_{rec} is the power received by an antenna located in the working volume, <.> refers to the ensemble averaging over N samples during a stirrer rotation, η_{Tx}, η_{Rx} are the antenna efficiencies of the adopted antennas, λ is the wavelength and V is the volume of the RC.

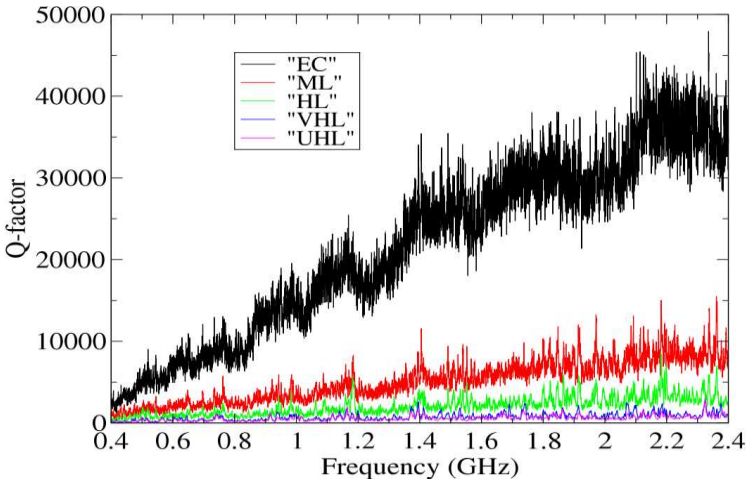

Figure 6: Quality factor of the reproduced scenarios that are reported in Table II. EC means "empty chamber", ML means "medium load", HL means "High load", VHL means "very high load", and UHL means "ultra high load". They are obtained by loading the RC with absorbing material [29], [37], Table I.

Table I: The different RC loading conditions are achieved by adding absorbing materials provided by Emerson & Cuming.

	VHP-18-NRL	VHP-8-NRL	ANW-77
ML	0	2	0
HL	0	2	5
VHL	4	8	4
UHL	4	10	8

The corresponding K factor values are reported in Fig. 7.

,

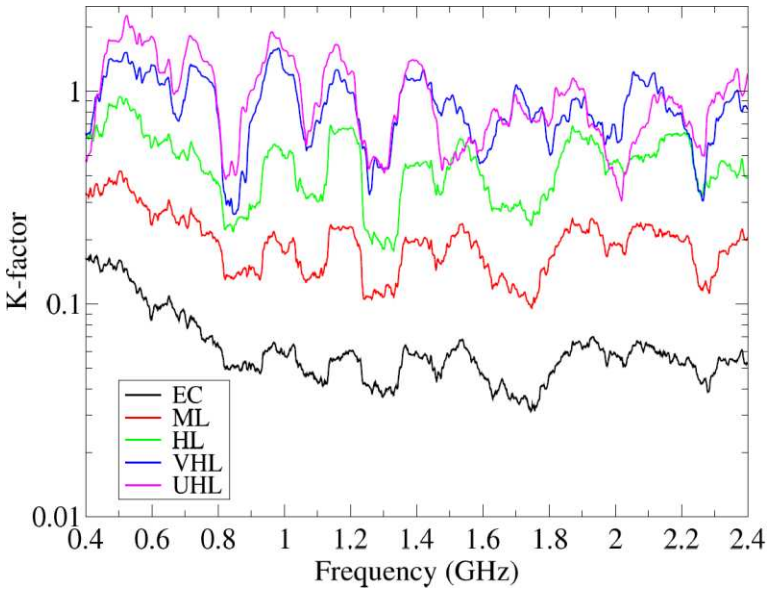

Figure 7: K-factor of the reproduced scenarios. A sliding window over 400 frequency point has been applied to better highlight differences among the various loading conditions.

It is therefore clear how an RC can be tuned to replicate a real situation. Other parameters of interest for the characterization of a wireless propagating environment are the power delay profile (PDP), the time delay spread τ, and the coherence bandwidth B_c.
The PDP is obtained by averaging the impulse response of the chamber *h(t)* over the *N* stirrer rotation.

$$PDP(t) = \langle |h(t)|^2 \rangle_N \tag{7}$$

The PDP describes the energy decay in the propagation environment. The first and second moments, corresponding to average delay spread (τ_{ave}) and root mean square delay spread (τ_{rms}) respectively, are useful parameters to describe propagation conditions [42]

$$\tau_{ave} = \frac{\int_0^\infty tPDP(t)dt}{\int_0^\infty PDP(t)dt} \tag{8}$$

$$\tau_{RMS} = \frac{\int_0^\infty (t-\tau_{ave})^2 PDP(t)dt}{\int_0^\infty PDP(t)dt}\,. \tag{9}$$

A similar definition is possible in the spectral domain, which leads to the coherence bandwidth of the wireless propagation channel [43]. A well operated RC develops ergodicity that would result in a band-pass filtering effect given by the Lorentzian response of the RC cavity. The connection between the width of the Lorentzian and the average coherence bandwidth of a wireless channel has been explored in [44], also accounting for the non-uniform spectral overlap of the cavity resonances as mechanical mode tuning is performed to create dynamical multi-path fading. This creates a deviation from the Lorentzian response that is more pronounced for low modal overlapping, which is reported in Fig. 8, where the probability density function of the coherence bandwidth is parameterized with the average number of overlapping environment resonances. Figure 8 is extracted from [44] by courtesy of the authors. The dependence of the local number of overlapping resonances has a non-trivial dependence on frequency and losses [45].

,

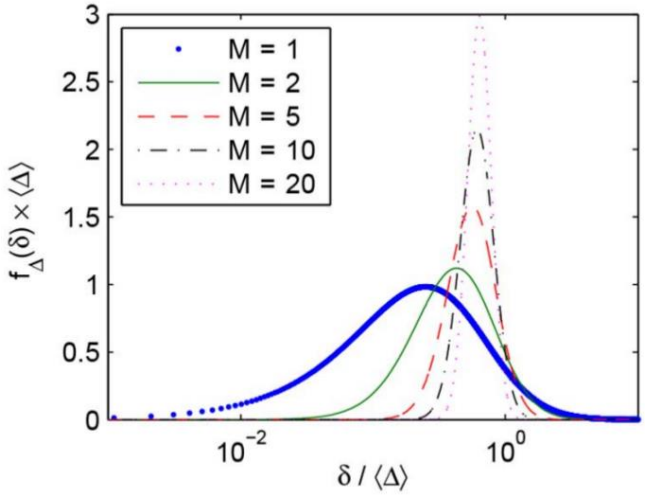

Figure 8: Normalized probability density function of δ/Δ for M cavity modes (Curtesy from [44]).

Figure 9 shows the PDP which is tunable by adding absorbers within the RC, Table I. Those absorbers can be placed both on the floor and on the walls. Their number and placement differently affect the overall behavior of the RC [37], [46]. It is therefore clear how an RC can be tuned to replicate a real situation.

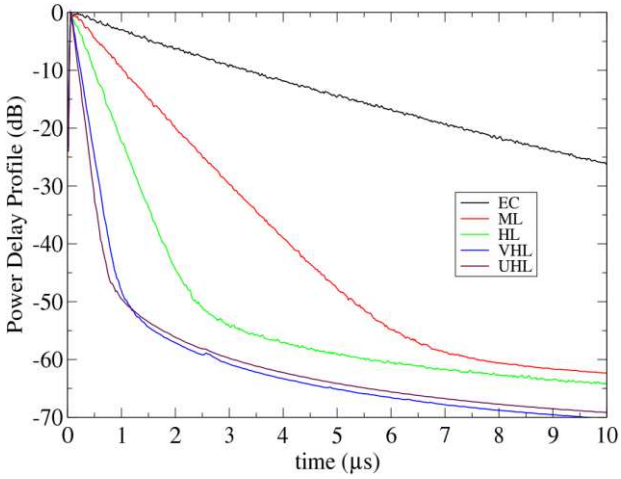

Figure 9: Power delay profile for the reproduced scenarios. They are obtained by loading the RC with absorbing material [29], [37], Table I.

,

The time delay spread obtained in the RC, many are reported in Table II, are comparable to those recommended by the standard for the laboratory replication of typical environments [47].

Table II: Time delay spread of the emulated scenarios.

Scenario	Time delay spread (ns)
Empty chamber (EC)	1347
Medium load (ML)	370
High load (HL)	163
Very high load (VHL)	67
Ultra high load (UHL)	54

The coherence bandwidth B_c is a frequency domain parameter which define the band over which frequency component experiences to the same propagation conditions and similar fading. It is directly related to the root mean square delay spread [39], [48]-[49]. On the contrary, in case of large band communications such as the 4G or 5G LTE signals, the usage of very large bandwidth exposes many channel carriers to very different fading conditions because their distance is larger than B_c. Figure 10 reports the computed B_c values for the above described RC loading conditions.

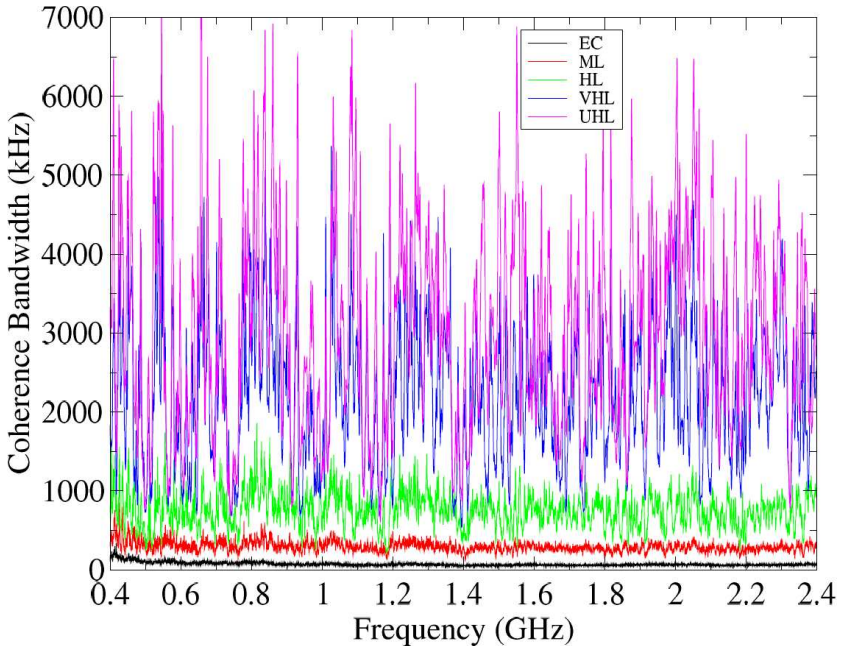

Figure 10: Coherence bandwidth for the reproduced scenarios that are reported in Table II. They are obtained by loading the RC with absorbing material.

,

Finally, the measurement uncertainty inside an RC is a well assessed issue [3]. In particular, it is related to the number of statistical uncorrelated chamber realizations which depends on stirrer geometry and efficiency [50], [51]. For our chamber, and for the adopted measurement conditions, the residual uncertainty is less than +/- 1 dB.

4. TESTING OF REAL OPERATING BASE STATIONS

As anticipated above, the RC has been used to replicate real propagation conditions of a 4G LTE cellular network and verify their impacts (synthesized through tuning the RC parameters mentioned above) over the performances perceived by the end user. A 4G LTE base station (here after also referred as an evolved-nodeB, (eNB) has been connected to a radio antenna transmitting inside a reverberation chamber as described in chapter 3. In order to verify the impacts of the replicated propagation environments on LTE performances, first of all some key performance indicators (KPIs) should be considered as a metric to measure the user's perception of quality. As the LTE technology is entirely packet-switched (that means: no permanent connection between two end points: the resources are assigned as the packets run through the network, following an on-demand approach) the most important of these KPIs is throughput, to be measured both in uplink (from UE to network) and downlink (from network to UE). This applies specially to wideband LTE non real time bearers (which support applications like FTP, web browsing, mails, etc.) where the entire cell bandwidth, or a big part of this, could be used by a single UE. A standard LTE terminal may use indeed up to the entire bandwidth configured for the serving cell, 20 MHz or more, if connectivity through multiple carriers - so called carrier aggregation (CA) - is supported. Nevertheless, the LTE technology is also designed and specified by 3GPP to support also the transmission of internet of things (IoT) applications, which require, in contrast, a very limited band to support the machine-to-machine communication and the transmission of few bytes of data toward sensors and smart-meters. In this case, the most important KPIs are service availability, battery draining, round trip time (RTT), and packet loss. Voice over LTE (VoLTE), and video over LTE (ViLTE) services (as opposed to other technologies like 2G (GSM) and 3G (UMTS) when implemented in LTE are also packet-switched. For these kinds of services, the most relevant KPI is the dropped-call rate (DCR) and the perceived quality of voice, or mean opinion score (MOS). The MOS provide the level of intelligibility on a scale from five (excellent) to one (very poor). All these KPIs are summarized in Table III.

Table III - main KPIs for the evaluation of the LTE performances in RC.

Bearer	Relevant KPIs
Non real time wideband	Throughput [Mbps]
Non real time narrowband (IoT)	Service availability [%] RTT [ms] packet loss [%]
VoLTE, ViLTE	DCR [%] MOS [1,..,5]

Another topic to be considered when testing cellular networks is the impact of the propagation environment over the quality of the radio signal. To exploit this, several parameters have been defined to provide metrics for the evaluation of radio quality. Certainly, these parameters could be considered also when a radio signal propagates inside a reverberation chamber:

- received signal strength indicator (RSSI) is the total wideband power received by the UE (in downlink direction) or by the base station (in uplink direction). It includes all possible contributions to the received signal, included pilot symbols, traffic, interference and noise;
- reference signal received power (RSRP) is the average power of the pilot symbols of the LTE signal transmitted in downlink direction (to the UE). Additional information can be found in [52]; as these symbols are spread throughout the whole band, this indicator could be meant as a measure of the power spectral density of the LTE signal, as it is received by the UE, when no other traffic is present;

,

- reference signal received quality (RSRQ) is the ratio between RSRP (scaled-up to the entire bandwidth) and the RSSI. Thus, it provides indications on the amount of cell load. See [52] for further details;
- signal to interference noise ratio (SINR) is the ratio between the wanted part of the signal and the sum of interference and noise;
- channel quality indications (CQI) dimensionless measurement of air interface quality performed by UE and reported to the base station for link adaptation purposes;
- block error rate (BLER) is the rate of transport blocks received with errors, or never received, which are negatively acknowledged by the UE in an automatic request for re-transmission process (HARQ);
- modulation and coding schemes (MCS). The LTE BS decide how much a transport block transmission should be protected based on feedback received by the UE and BLER requirements. The higher is the protection of one TB, the more robust is the transmission, but the lower is the amount of information that could be sent on it. The protection level, together with the chosen modulation, identify the modulation and coding scheme [29]-[30] concept, which is defined for each transport block that is transmitted.

Those parameters will be used to better quantify the impact of multipath propagation on performance. For example, the insertion of absorbing panels causes a reduction on the RSRP as part of the energy is absorbed. If different multipath conditions are set up via the introduction/removal of absorbing material, one good approach is to compensate the introduced variation in RSRP via attenuators, in order to run the tests at different multipath conditions, but with same RSRP level, isolating this way the unique effect of multipath. This approach has been followed during a test campaign where two different loading conditions were envisioned for the RC: in the first condition, the RC was empty, so a totally reflecting resonant enclosure (empty load in the picture below). In the second case, the chamber was filled with some absorbing panels, in order to reduce the amount of multipath, reaching a loading condition referred as "high load" in Fig. 11:

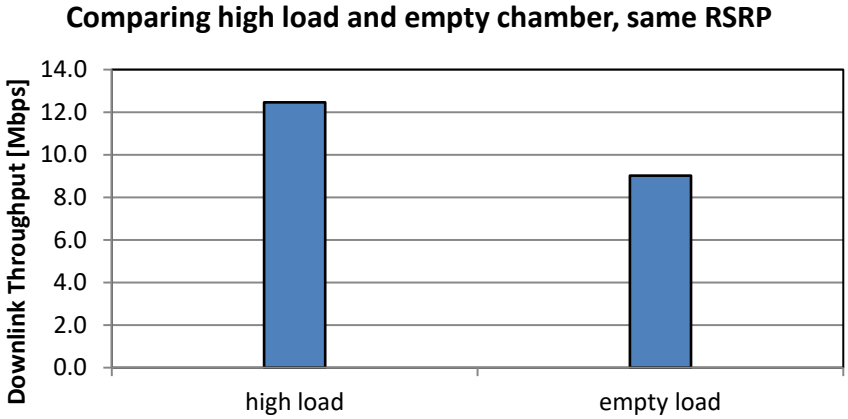

Figure 11: Downlink throughput measured at RSRP = -105 dBm, with high load (typical multipath for indoor propagation) and empty chamber (very rich multipath).

The reason of the low throughput is the poor radio signal condition where the test has been executed (RSRP = -105 dBm). This high load condition is proven to replicate the same propagation condition (Q-factor, power-delay-profile, K-Rician factor, and coherence bandwidth) of a typical cellular network radiating in outdoor environment and was obtained by inserting 2 absorbing anechoic panels + 5 absorbing planar panels as referred in Figs. 6, 7, 9, 10.

From the picture, it is noticeable the effect of an environment rich in multipath on the overall throughput performances, while maintaining the same signal strength (RSRP). Multipath cause a throughput reduction from 12.5 Mbps down to 9 Mbps - almost 30%.

Similar study could be performed for the uplink direction, where the UE sends data to the eNB, which sends data to the eNB, which receives it using different reception diversity schemes. One of the most efficient reception schemes is the coordinated multipoint, where the UE transmits toward a serving cell and a neighbor,

,

non-serving cell, and the signal received by the neighbor cell (that would be normally treated as interference) is combined with the signal received by the serving cell in order to maximize the SINR. The concept is expressed in Fig. 12: in this scenario, the neighbor cell is also called "helper cell", as it gather its contribution of the signal transmitted by the UE and sends it to the serving cell for a final combining.

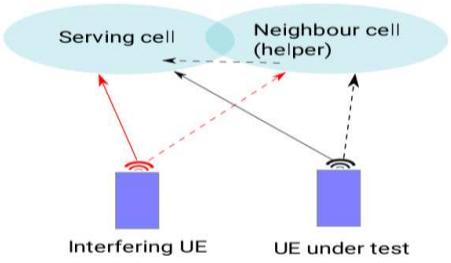

Figure 12: Coordinated multipoint concept.

It should be highlighted that both cells already implement their own reception scheme which is based on diversity. For a single cell, normally two types of reception schemes exist: the Maximum Ratio Combining (MRC), which is unaware of interference, thus it is aimed to increase the signal-to-noise ratio, without capabilities in interference-rejection, and the interference rejection combining (IRC) which is able to equalize the interference if it comes from well defined directions. The coordinated multipoint reception is built "on top" of this latter reception scheme to provide a benefit on the SINR of the combined signal. More details are reported in [29].

Its benefit is visible in Figs. 13 and 14, where an interference has been generated in RC through a second UE, transmitting toward the eNB and progressively increasing its power.

Figure 13 shows the impact on uplink throughput of an interference generated by a second UE camped on another cell radiating in RC. Its power is progressively increased by means of electronic arrays, starting from an initial value, generating interference on the serving cell of UE under test. As expected, the coordinated multipoint demonstrated to be more robust than other simpler reception schemes. This highlight the relevance of cell coordination in interference rejection.

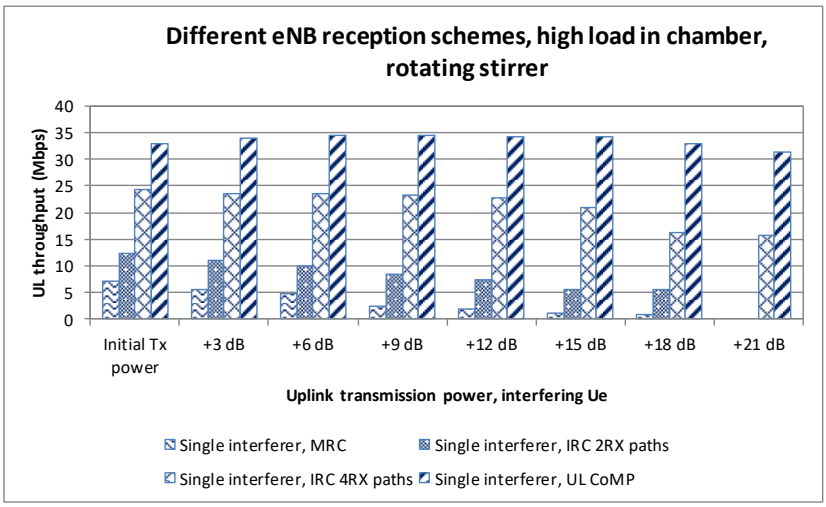

Figure 13: Effect of interferer over the uplink LTE performances in RC, high-load in chamber (replicating outdoor propagation) vs different reception schemes.

,

In Fig. 14, the uplink throughput with coordinated multipoint enabled on the eNB, comparing the high load condition with the empty chamber condition, which is much richer in multipath. In Fig. 11, for the downlink, the two chamber conditions have been tested at the same value of radio signal (RSRP) present in chamber in order to isolate exclusively the effect of multipath. It is shown that there is an evident impact of multipath over the uplink performance, and such impact is even more evident the bigger the interference is. As the previous example, this demonstrate how the multipath may affect the performance perceived by the user. The coordinated multipoint is part of the bunch of features brought by 3GPP and also known as LTE-Advanced (LTE-A) solutions. They are meant to boost the performances of each single user to reach the highest throughput possible. One of these is CA: with this feature, the resources of two (or more) overlapping cells, transmitting at different frequencies and different bands, are joined together to allow a single user to reach bit-rates even equal or higher than 1 Gbps. The CA is possible also in the uplink direction, however, in this case the single user maximum bit rate is lower.

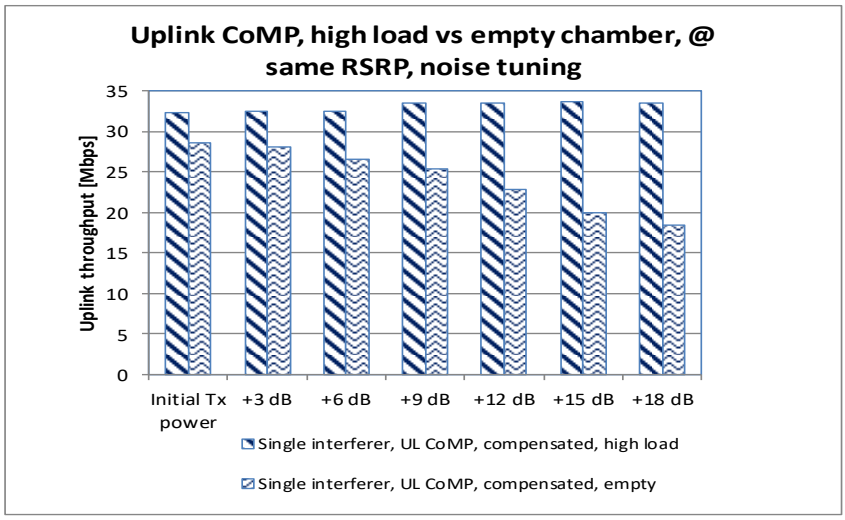

Figure 14: Uplink LTE performances when coordinated multipoint is used, comparing high load (HL) setup in RC with empty chamber (EC).

Figure 15 shows the aggregated throughput when an UE, 64-QAM modulation capable, is simultaneously connected to a primary cell (10 MHz bandwidth, 1800 MHz band) and a secondary cell (10 MHz bandwidth, 800 MHz band) organized in a carrier CA pair.

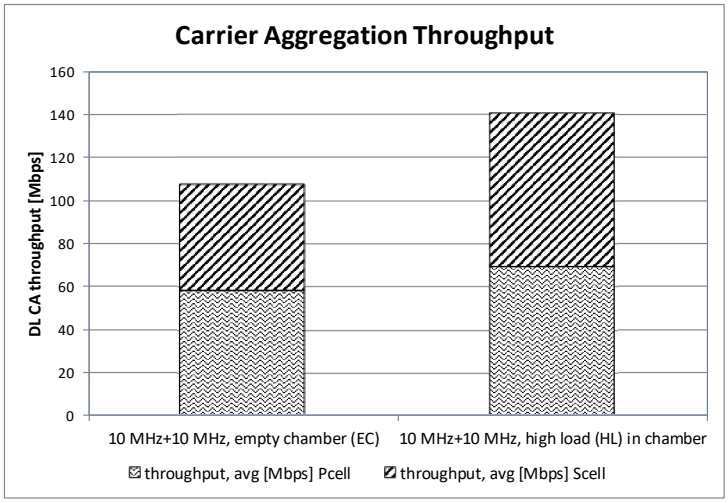

Figure 15: Downlink LTE carrier aggregation performances for a UeE connected simultaneously two cells (one primary and one secondary), 10 MHz + 10 MHz bandwidth, 64-QAM modulation.

,

The effect of multipath is similar to the one presented in Fig. 10 and could be quantified on a level of 30% of impairment introduced by multipath.

Further details regarding CA performances in RC are reported in [53]. Looking at previous examples, one could be induced to think that fourth generation LTE cellular networks are all about throughput, but it's not like that. The access is entirely packet-switched; thus voice is also carried over a packet-switched bearer. The solution is called VoLTE and its quality is based on MOS. Figure 16 shows the result of a test campaign where the VoLTE quality has been measured for different types of mobile to mobile calls (both UE camped on 4G, which deal to a 23.85 Kbps AMR codec rate, 4G to 3G call, which deal to a 12.65 Kbps AMR codec rate, and 4G to 2G call, which deal to an 8 Kbps AMR codec rate). From the picture it is evident that, even at very low signal level, performance in terms of MOS are always acceptable, until radio-link failure does not occur and the call is finally dropped. Contrary to the throughput, there is not a linear relation between multipath and MOS. Instead, the MOS is mainly polarized by the codec rate that is chosen by the network.

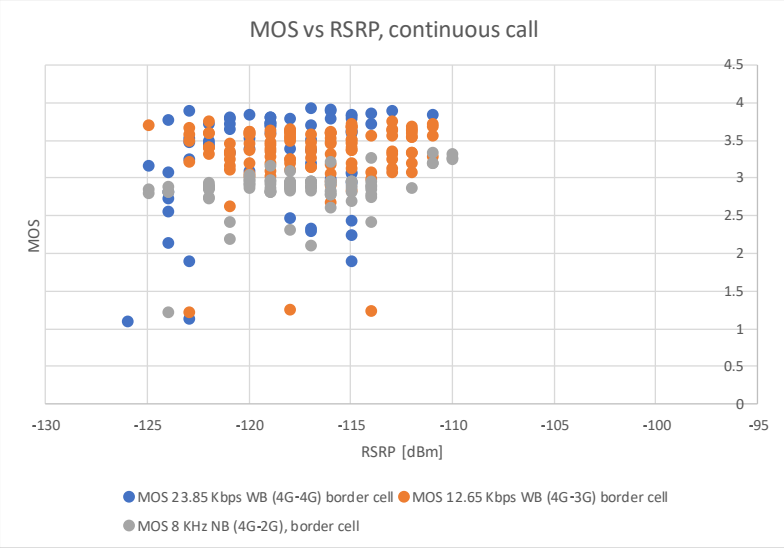

Figure 16: Mean opinion score for VoLTE in reverberation chamber, for different AMR codec.

5. CONCLUSION

The use of the reverberation chamber to emulate both indoor and outdoor wireless propagation channels is a flexible and reliable method to perform robust OTA testing of high data rate wireless devices for 4G LTE and 5G mobile networks. The method has been enhanced through the use of a base station connected to the live network of the Telecom operator: this allows for creating truly real-life signals received by the user equipment. The reverberation chamber supports multiple reflections that results in a multipath faded signal stressing onto the device under test.
According to the propagation environment to be emulated, the multipath degree can be easily tuned by varying the amount and the position of the loading lossy material and the antenna orientation.
Signal-to-noise ratio and throughput of the data received by commercial user equipment devices can thus be tested and predicted in realistic propagation conditions.

References

[1] D. A. Hill, “Plane wave integral representation for fields in reverberation chambers,” IEEE Trans. Electromagn. Compat., vol. 40, no. 3, pp. 209– 217, Aug. 1998.
[2] P. Corona, G. Ferrara, and M. Migliaccio, “Reverberating chambers as sources of stochastic electromagnetic fields,” IEEE Trans. on EMC., vol. 38, no. 3, pp. 348–356, Aug. 1996.
[3] Electromagnetic compatibility (EMC) - Part 4-21: Testing and measurement techniques - Reverberation chamber test methods, 2nd ed., International Standards - IEC 61000-4-21, Geneva, Switzerland, Apr. 2011.

,

[4] G. Gradoni, D. Micheli, F. Moglie, and V. Mariani Primiani, "Absorbing cross section in reverberation chamber: experimental and numerical results," Progress in Electromagnetics Research B, Vol. 45, 187-202, 2012.
[5] D. Micheli et al., "Shielding effectiveness of carbon nanotube reinforced concrete composites by reverberation chamber measurements," 2015 International Conference on Electromagnetics in Advanced Applications (ICEAA), Turin, 2015, pp. 145-148.
[6] V. Mariani Primiani and F. Moglie, "Numerical simulation of LOS and NLOS conditions for an antenna inside a reverberation chamber," J. Electromagn. Waves Appl., vol. 24, no. 17/18, pp. 2319–2331, 2010.
[7] A. Sorrentino, G. Ferrara, A. Gifuni, and M. Migliaccio, "Antenna pattern in a multipath environment emulated in a reverberating chamber," in Proc. IEEE 7th EuCAP, Gothenburg, Sweden, Apr. 2013, pp. 3561–3565.
[8] F. Moglie, V. Mariani Primiani, and A. P. Pastore, "Modeling of the human exposure inside a random plane wave field," Progress In Electromagnetics Research B, Vol. 29, 251-267, 2011.
[9] E. Genender, C. L. Holloway, K. A. Remley, J. M. Ladbury, G. Koepke,and H. Garbe, "Simulating the multipath channel with a reverberation chamber: Application to bit error rate measurements," IEEE Trans. Electromagn. Compat., vol. 52, no. 4, pp. 766–777, Nov. 2010.
[10] H. Fielitz, K. A. Remley, C. L. Holloway, Q. Zhang, Q. Wu, and D. W. Matolak, "Reverberation-chamber test environment for outdoor urban wireless propagation studies," IEEE Antennas Wireless Propag. Lett., vol. 9, pp. 52–56, 2010.
[11] C. L. Holloway, D. A. Hill, J. M. Ladbury, P. F. Wilson, G. Koepke, and J. Coder, "On the use of reverberation chambers to simulate a Rician radio environment for the testing of wireless devices," IEEE Trans. Antennas Propag., vol. 54, no. 11, pp. 3167–3177, Nov. 2006.
[12] G. B. Tait and R. E. Richardson, "Wireless channel modeling of multiply connected reverberant spaces: Application to electromagnetic compatibility assessment," IEEE Trans. Electromagn. Compat., vol. 55, no. 6, pp. 1320–1327, Dec. 2013.
[13] J. S. Giuseppe, C. Hager, and G. B. Tait, "Wireless RF energy propagation in multiply-connected reverberant spaces," IEEE Antennas Wireless Propag. Lett., vol. 10, pp. 1251–1254, 2011.
[14] K. Rosengren and P.-S. Kildal, "Radiation efficiency, correlation, diversity gain, and capacity of a six monopole antenna array for a MIMO system: Theory, simulation and measurement in reverberation chamber," Proc. Inst. Elect. Eng.—Microw., Antennas Propag., vol. 152, no. 1, pp. 7–16, Feb. 2005.
[15] J. B. Coder, J. M. Ladbury, C. L. Holloway, and K. A. Remley, "Examining the true effectiveness of loading a reverberation chamber: How to get your chamber consistently loaded," in Proc. IEEE Int. Symp. Electromagn. Compat., Fort Lauderdale, FL, USA, Jul. 2010, pp. 530–535.
[16] C. Orlenius, M. Franzén, P.-S. Kildal, and U. Carlberg, "Investigation of heavily loaded reverberation chamber for testing of wideband wireless units," in Proc. IEEE Antennas Propag. Soc. Int. Symp., Albuquerque, NM, USA, Jul. 2006, pp. 3569–3572.
[17] V. Mariani Primiani and F. Moglie, "Numerical simulation of reverberation chamber parameters affecting the received power statistics," IEEE Trans. Electromagn. Compat., vol. 54, no. 3, pp. 522–532, Jun. 2012.
[18] F.Moglie and V.Mariani Primiani, "Analysis of the independent positions of reverberation chamber stirrers as a function of their operating conditions," IEEE Trans. Electromagn. Compat., vol. 53, no. 2, pp. 288–295, May 2011.
[19] X. Chen, "Measurement uncertainty of antenna efficiency in a reverberation chamber," IEEE Trans. Electromagn. Compat., vol. 55, no. 6, pp. 1331–1334, Dec. 2013.
[20] C. M. J. Wang et al., "Parameter estimation and uncertainty evaluation in a low Rician K-factor reverberation-chamber environment," IEEE Trans. Electromagn. Compat., vol. 56, no. 5, pp. 1002–1012, Oct. 2014.
[21] K. A. Remley, R. J. Pirkl, H. A. Shah, and C.-M. Wang, "Uncertainty from choice of mode-stirring technique in reverberation-chamber measurements," IEEE Trans. Electromagn. Compat., vol. 55, no. 6, pp. 1022–1030, Dec. 2013.
[22] F. Moglie and V. Mariani Primiani, "Numerical analysis of a new location for the working volume inside a reverberation chamber," IEEE Trans. Electromagn. Compat., vol. 54, no. 2, pp. 238–245, Apr. 2012.
[23] P.-S. Kildal, X. Chen, C. Orlenius, M. Franzén, and C. S. L. Patané, "Characterization of reverberation chambers for OTA measurements of wireless devices: Physical formulations of channel matrix and new uncertainty formula," IEEE Trans. Antennas Propag., vol. 60, no. 8, pp. 3875–3891, Aug. 2012.
[24] D. Micheli, M. Barazzetta, R. Diamanti, P. Obino, R. Lattanzi, L. Bastianelli, V. Mariani Primiani and F. Moglie, "Over-the-Air Tests of High-Speed Moving LTE Users in a Reverberation Chamber," in IEEE Transactions on Vehicular Technology, vol. 67, no. 5, pp. 4340-4349, May 2018. doi:

,

10.1109/TVT.2018.2795650 URL: http://ieeexplore.ieee.org/stamp/stamp.jsp?tp=&arnumber=8264800&isnumber=8357823
[25] R. Recanatini, F. Moglie, and V. Mariani Primiani, “Performance and immunity evaluation of complete WLAN systems in a large reverberation chamber,” IEEE Trans. Electromagn. Compat., vol. 55, no. 5, pp. 806–815, Oct. 2013.
[26] A. Hussain and P.-S. Kildal, “Study of OTA throughput of 4G LTE wireless terminals for different system bandwidths and coherence bandwidths in rich isotropic multipath,” in Proc. 7th EuCAP, Gothenburg, Sweden, Apr. 2013, pp. 312–314.
[27] D. Micheli, M. Barazzetta, F. Moglie and V. Mariani Primiani, "Power Boosting and Compensation During OTA Testing of a Real 4G LTE Base Station in Reverberation Chamber," in IEEE Transactions on Electromagnetic Compatibility, vol. 57, no. 4, pp. 623-634, Aug. 2015.
[28] M. Barazzetta, D. Micheli, F. Moglie and V. Mariani Primiani, "Over-the-air performance testing of a real 4G LTE base station in a reverberation chamber," 2014 IEEE International Symposium on Electromagnetic Compatibility (EMC), Raleigh, NC, 2014, pp. 903-908. doi: 10.1109/ISEMC.2014.6899096 URL: http://ieeexplore.ieee.org/stamp/stamp.jsp?tp=&arnumber=6899096&isnumber=6898924
[29] M. Barazzetta, D. Micheli, L. Bastianelli, R. Diamanti, M. Totta, P. Obino, R. Lattanzi, F. Moglie, and V. Mariani Primiani, “A comparison between different reception diversity schemes of a 4G-LTE base station in reverberation chamber: a deployment in a live cellular network,” IEEE Trans. Electromagn. Compat., vol. 59, no. 6, Dec. 2017, accepted for pubblication, DOI: 10.1109/TEMC.2017.2657122.
[30]D. Micheli, M. Barazzetta, R. Diamanti, P. Obino, R. Lattanzi, L. Bastianelli, V. Mariani Primiani, and F. Moglie, “Over-the-Air Tests of High-Speed Moving LTE Users in a Reverberation Chamber," in IEEE Transactions on Vehicular Technology, vol. 67, no. 5, pp. 4340-4349, May 2018.
[31] M. Barazzetta, D. Micheli, P. Gianola, F. Moglie and V. Mariani Primiani, "4G-LTE base station output power estimation from statistical counters during over-the-air tests in reverberation chamber," 2014 International Symposium on Electromagnetic Compatibility, Gothenburg, 2014, pp. 284-289. doi: 10.1109/EMCEurope.2014.6930918 URL: http://ieeexplore.ieee.org/stamp/stamp.jsp?tp=&arnumber=6930918&isnumber=6930855
[32] Mischa Schwarts, “Mobile Wireless Communications”, Columbia University, New York, Jan. 2005
[33] X. Chen, P.-S. Kildal, and S.-H. Lai, “Estimation of average Rician K-factor and average mode bandwidth in loaded reverberation chamber,” IEEE Antennas Wireless Propag. Lett., vol. 10, pp. 1437–1440, 2011.
[34] M. Panitz and D. C. Hope, “Characteristics of wireless systems in resonant environments,” in IEEE Electromagnetic Compatibility Magazine, vol. 3, no. 3, pp. 64-75, 3rd Quarter 2014, doi: 10.1109/MEMC.2014.6924331
[35] ETSI TS 136 104, "LTE; Evolved Universal Terrestrial Radio Access (E-UTRA); User Equipment (UE) radio transmission and reception", V10.3.0 (2011-06).
[36] F. Moglie, G. Gradoni, L. Bastianelli and V. Mariani Primiani, "A mechanical mode-stirred reverberation chamber inspired by chaotic cavities," *2015 IEEE Metrology for Aerospace (MetroAeroSpace)*, Benevento, 2015, pp. 437-441. doi: 10.1109/MetroAeroSpace.2015.7180697 URL:http://ieeexplore.ieee.org/stamp/stamp.jsp?tp=&arnumber=7180697&isnumber=7180612
[37] L. Bastianelli, L. Giacometti, V. Mariani Primiani and F. Moglie, "Effect of absorber number and positioning on the power delay profile of a reverberation chamber," *2015 IEEE International Symposium on Electromagnetic Compatibility (EMC)*, Dresden, 2015, pp. 422-427. doi: 10.1109/ISEMC.2015.7256199 URL:http://ieeexplore.ieee.org/stamp/stamp.jsp?tp=&arnumber=7256199&isnumber=7256113
[38] R. Serra *et al*., "Reverberation chambers a la carte: An overview of the different mode-stirring techniques," in *IEEE Electromagnetic Compatibility Magazine*, vol. 6, no. 1, pp. 63-78, First Quarter 2017. doi: 10.1109/MEMC.2017.7931986 URL:http://ieeexplore.ieee.org/stamp/stamp.jsp?tp=&arnumber=7931986&isnumber=7931808
[39] R. Serra, "Reverberation chambers through the magnifying glass: an overview and classification of performance indicators," in *IEEE Electromagnetic Compatibility Magazine*, vol. 6, no. 2, pp. 76-88, Second Quarter 2017. doi: 10.1109/MEMC.0.7990003 URL:http://ieeexplore.ieee.org/stamp/stamp.jsp?tp=&arnumber=7990003&isnumber=7989980
[40] C. L. Holloway, D. A. Hill, J. M. Ladbury and G. Koepke, "Requirements for an effective reverberation chamber: unloaded or loaded," in *IEEE Transactions on Electromagnetic Compatibility*, vol. 48, no. 1, pp. 187-194, Feb. 2006. doi:

,

10.1109/TEMC.2006.870709URL: http://ieeexplore.ieee.org/stamp/stamp.jsp?tp=&arnumber=1614052&isnumber=33884
[41] J. Ladbury, G. Koepke and D. Camell, “Evaluation of the NASA Langley research center mode-stirred chamber facility,” National Institute of Standards and Technology, Tech. Rep. NIST TN – 1508, Jan. 1999
[42] E. Genender, C. L. Holloway, K. A. Remley, J. M. Ladbury, G. Koepke and H. Garbe, "Simulating the Multipath Channel With a Reverberation Chamber: Application to Bit Error Rate Measurements," in *IEEE Transactions on Electromagnetic Compatibility*, vol. 52, no. 4, pp. 766-777, Nov. 2010. doi: 10.1109/TEMC.2010.2044578
URL:http://ieeexplore.ieee.org/stamp/stamp.jsp?tp=&arnumber=5446379&isnumber=5580183
[43] Rappaport, Theodore S. *Wireless Communications: Principles and Practice*. Upper Saddle River, N.J: Prentice Hall PTR, 2002.
[44] L. R. Arnaut and G. Gradoni, "Probability Distribution of the Coherence Bandwidth of a Reverberation Chamber," in *IEEE Transactions on Antennas and Propagation*, vol. 63, no. 5, pp. 2286-2290, May 2015. doi: 10.1109/TAP.2015.2403398
[45] G. Gradoni, V. Mariani Primiani and F. Moglie, "Dependence of reverberation chamber performance on distributed losses: A numerical study," 2014 IEEE International Symposium on Electromagnetic Compatibility (EMC), Raleigh, NC, 2014, pp. 775-780. doi: 10.1109/ISEMC.2014.6899073 URL: http://ieeexplore.ieee.org/stamp/stamp.jsp?tp=&arnumber=6899073&isnumber=6898924
[46] Bradley, David T., and Lily M. Wang. "Quantifying the double slope effect in coupled volume room systems." Building Acoustics 16.2 (2009): 105-123.
[47] Guidelines for evaluation of radio interface technologies for IMT-Advanced, International Telecommunication Union - ITU Report M.2135-1, Dec. 2009.
[48] C. L. Holloway, H. A. Shah, R. J. Pirkl, K. A. Remley, D. A. Hill and J. Ladbury, "Early Time Behavior in Reverberation Chambers and Its Effect on the Relationships Between Coherence Bandwidth, Chamber Decay Time, RMS Delay Spread, and the Chamber Buildup Time," in *IEEE Transactions on Electromagnetic Compatibility*, vol. 54, no. 4, pp. 714-725, Aug. 2012. doi: 10.1109/TEMC.2012.2188896
URL:http://ieeexplore.ieee.org/stamp/stamp.jsp?tp=&arnumber=6174465&isnumber=6266739
[49] X. Chen, P. Kildal, C. Orlenius and J. Carlsson, "Channel Sounding of Loaded Reverberation Chamber for Over-the-Air Testing of Wireless Devices: Coherence Bandwidth Versus Average Mode Bandwidth and Delay Spread," in *IEEE Antennas and Wireless Propagation Letters*, vol. 8, pp. 678-681, 2009. doi: 10.1109/LAWP.2009.2025149
URL:http://ieeexplore.ieee.org/stamp/stamp.jsp?tp=&arnumber=5072260&isnumber=4808186]
[50] A. Gifuni, L. Bastianelli, M. Migliaccio, F. Moglie, V. Mariani Primiani and G. Gradoni, "On the Estimated Measurement Uncertainty of the Insertion Loss in a Reverberation Chamber Including Frequency Stirring," in IEEE Transactions on Electromagnetic Compatibility, vol. 61, no. 5, pp. 1414-1422, Oct. 2019. doi: 10.1109/TEMC.2018.2870073
[51] L. R. Arnaut, "Measurement uncertainty in reverberation chambers – I. Sample statistics", NPL report, pp. 1-136, Dec. 2008.
[52] “LTE; evolved universal terrestrial radio access (E-UTRA); physical layer procedures,” ETSI, Sophia Antipolis Cedex, France, 3GPP Technical Specification TS 36.213 V8.8.0, Oct. 2009.
[53] D. Micheli, M. Barazzetta, C. Carlini, R. Diamanti, V. Mariani Primiani and F. Moglie, "Testing of the Carrier Aggregation Mode for a Live LTE Base Station in Reverberation Chamber," in IEEE Transactions of Vehicular Technology, vol. 66, no. 4, pp. 3024-3033, April 2017.

,